論　文

表面科学 Vol. 16, No. 7, pp. 441–447, 1995

Initial Stage Growth and Electronic Structure of Al Overlayer on a Single-Domain Si(001)2×1 Surface†

Han Woong YEOM, Tadashi ABUKAWA*, Yuji TAKAKUWA*, Masashi NAKAMURA*, Mitsuyuki KIMURA*, Akito KAKIZAKI**, Shoji SUZUKI, Shigeru SATO and Shozo KONO*

Department of Physics, Faculty of Science, Tohoku University, Sendai 980–77
*Research Institute for Scientific Measurements, Tohoku University, Sendai 980–77
**Synchrotron Radiation Laboratory, Institute for Solid State Physics, The University of Tokyo Roppongi, Tokyo 106

(Received February 20, 1995 : Accepted April 7, 1995)

Initial stage growth and electronic structures of Al overlayer on a wide-terrace single-domain Si(001)2×1 surface has been studied by low-energy-electron-diffraction (LEED) and photoelectron spectroscopy. The sequences of 2D phases found by LEED for Al coverages ≤ 0.5 ML at RT and 300°C are interpreted on the basis of an order-disorder transition of arrays of one-dimensional Al-dimer chains. The detailed electronic structure of 2×2 phase formed at ~0.5 ML has been studied by angle-resolved photoelectron spectroscopy (ARPES) using synchrotron radiation. The existence and dispersions of five different surface states are identified for the first time, one at binding energies a little less than 1 eV and the others between 1 and 2 eV. The origin of the surface states can be interpreted in terms of the Al-dimer structures on Si(001).

1. Introduction

In recent years growth of group-III metals (Al, Ga and In) on Si(001) surfaces has become one of the most notable subjects in surface science due to its highly-anisotropic submonolayer growth and interesting adsorbate structure. It has been found by low-energy-electron-diffraction (LEED), reflection-high-energy-electron-diffraction (RHEED) and Auger-electron spectroscopy (AES) that the group-III metals grow basically in the Stranski-Krastanov (SK) mode on Si(001)[1~4]. A couple of two-dimensional (2D) phases were found during the initial stage growth before the formation of three-dimensional (3D) islands. By LEED[2~4] and scanning tunneling microscopy (STM)[5], it was suggested that the metal atoms initially form dimers and grow into long chains of dimers, which develop into 2×2 phases at a coverage of 0.5 ML (1ML = 6.8×10^{14} atoms/cm^2, the surface atomic density of a truncated Si(001)1×1 surface). However the growth modes toward and beyond the common 2×2 phase are different among the metal adsorbates. For Al adsorption the 2×2 phase has two different mode of formation depending on temperature and appears in a very wide range of coverage of > 0.35 ML at room temperature (RT)[4,5]. This makes a contrast to the cases of Ga and In adsorptions where only one mode of formation, but different each other, for 2×2 was reported and the 2×2 phases appear only in a narrow region of coverage around 0.5 ML[1~3]. A very local probe of STM showed little difference in the early stage (≦~ 0.5 ML) of growth of these metals[5]. This is not straightforwardly understood in the light of the differences among the adsorbates found by LEED and RHEED. Also for the growth above the coverage for 2×2 phase there remains several important questions, for example the coverage for the onset of island growth. Notably there is no 1×2 phase at coverages higher than ~0.5 ML for Al adsorption while 1×2 phases are reported for Ga and In adsorptions at ~1 ML[2,3]. The absence of 1×2 phase for Al adsorption contradicts the general notion that the substrate 2×1 phase would convert to a 1×2 phase at the 1 ML coverage of metal adsorbates. Therefore the details in growth mode of these metals on Si(001) deserve further study.

For the microscopic structure of the submonolayer phases, two possible models have been proposed, i.e., the so-called parallel and perpendicular dimer model, where the adsorbate dimers are parallel and perpendicular to the *unbroken* substrate Si dimers,

† 第14回表面科学講演大会（1994年11月30日～12月 2 日）にて発表

respectively[5]. Recent total energy calculations[6, 7], a tensor LEED study for Al and Ga adsorbates[8], an ion scattering spectroscopy (ISS) study for In adsorbate[9], a STM study for Al[10] and a X-ray standing wave (XSW) experiment for Ga[11] preferred the parallel dimer structure.

In contrast to quite a large amount of structural studies by LEED, ISS, XSW and STM on these surfaces, there are very few reports on the surface electronic structures. Angle-resolved photoelectron spectroscopy (ARPES) using a rare-gas resonant lamp was applied on a double-domain Si(001)2×2-In[7] and a single-domain Si(001)2×2-Ga and 2×3-Ga[12] surface, where a few surfaces states (SS's) were identified between Fermi level and 2 eV in binding energy (E_B). In the two previous studies, however, the dispersions of SS's could not be clearly determined and the origin of those SS's could not be understood. In a recent STM study[10] of the Al-induced 2×2 surface, the authors interpreted the STM image as an evidence for the existence of states due to Al-Si bond and Al-Al dimer-bond at 3 eV and −1 eV (an empty state) in binding energies, respectively, in disagreement with the ARPES result. These facts make it an urgent task to characterize in detail the surface electronic structure of the submonolayer phases of group-III metals on Si(001).

In this paper, we report LEED study and ARPES measurements using synchrotron radiation for the initial stage growth and electronic structure of Al overlayer on a wide-terrace single-domain (SD) Si(001)2×1 surface. The use of the wide-terrace SD surface is to avoid any ambiguity that would arise from the usual double-domain Si(001)2×1 surfaces. We also report the determination of absolute Al coverages for 2D phases including the 2×2 phase using an XPS intensity ratio (Al 2p/Si 2p) calibrated by a quartz thickness monitor. The present results clearly demonstrate that there is a general mode of growth for the adsorption of group-III metals on Si(001). Through detailed ARPES measurements using synchrotron radiation, we have identified, for the first time, five SS's inside the bulk band gap. The dispersions of the five SS's have been determined in detail. The origin of the SS's is discussed on the basis of the Al-dimer models of the surface.

2. Experimental

The experiments were performed in two different UHV spectrometer systems. LEED and XPS study was done at department of physics, Tohoku University, where a UHV photoelectron spectrometer (VG ADES-400) was used, which was equipped with LEED optics, a twin-anode X-ray source, a hemispherical electron-energy analyzer. ARPES measurements using synchrotron radiation was performed with another spectrometer (VG ADES-500) on the beam line BL-18A of Institute for Solid State Physics at Photon Factory, National Laboratory for High Energy Physics. The beam line is equipped with a constant-deviation-angle grazing-incidence monochromator. The overall angular and energy resolutions were ~ 1° and ~150 meV, respectively, at the used photon energies of 21.2 eV and 26.5 eV. The base pressure of both systems was ~3.0×10^{-11} mbar.

A mirror-polished Si-wafer ($25 \times 3.5 \times 0.38$ mm^3) was used as a substrate. The Si wafer was heated by direct resistive heating and its temperature was monitored by an infrared and an optical pyrometer. A wide-terrace single-domain Si(001)2×1 surface was prepared by preoxidation and cycles of *in situ* annealing and Si deposition[13]. The fraction of minor domain (1×2) was below 15% as determined from a ratio of LEED-spot intensities of the two domains measured by a spot photometer. Al was deposited onto the SD Si(001)2×1 surface held at RT from a pyrolytic boronnitride crucible heated by a W-filament. The Al source was thoroughly degassed to maintain the pressure during deposition below ~2.0×10^{-10}mbar. The absolute deposition rate of Al was determined by a quartz thickness monitor to be 0.23±0.04 ML/min. The amount of deposited Al on the RT surface was then determined from the duration of deposition and further monitored via XPS intensity ratios of Al 2p to Si 2p.

ARPES spectra were measured at a step of ~2° along various symmetric axes of the 2×2 surface Brillouin zone (SBZ, see Fig. 4f). We measured ARPES spectra not only along symmetric axes including the origin, $\bar{\Gamma}_{00}$, but also along symmetric axes excluding the origin, such as along $\bar{\Gamma}_{10}-\bar{\Gamma}_{11}$, $\bar{\Gamma}_{01}-\bar{\Gamma}_{11}$, $\bar{J}'_{00}-\bar{J}'_{10}$ and $\bar{J}_{00}-\bar{J}_{01}$ for a complete determination of SS-dispersions. ARPES spectra presented were taken with p-polarized synchrotron radiation of 21.2 eV at a 45°-incidence angle, unless otherwise stated.

3. Results and discussion

3.1 LEED and XPS study : initial stage growth

Figure 1 shows the change in XPS intensity ratio (Al 2p/Si 2p) and corresponding LEED patterns observed as a function of the duration of Al deposition. The deposited amount of Al in units of ML is also shown. For the as-deposited case, the XPS ratio grows linearly up to ~2 ML. This suggests that Al grows in a layer-by-layer fashion on the RT substrate, at least up to ~2 ML. After post-annealing (hereafter, the post-annealing means annealing at 300°C for 1.0 min after deposition, unless otherwise stated), the growth of XPS ratio changes its slope at ~1.0 ML. If we post-anneal the sample for an extended time, the XPS ratio decreases to a fixed value for the sample with deposited Al of ≧ 1 ML.

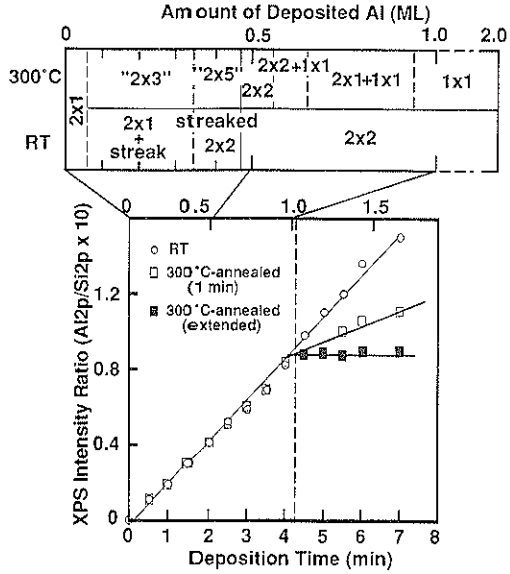

Fig. 1 Change in XPS intensity ratio (Al 2p/Si 2p) and the corresponding change of LEED pattern for the Al/Si(001) system as a function of the duration of Al deposition onto a single-domain Si(001)2×1 surface. The amount of deposited Al in ML is also specified. The circles represent the intensity ratios for deposition at RT. The intensity ratios after 300°C-annealing for 1 min (extended time) following deposition at RT are depicted with open (solid) squares. The solid lines are the results of linear fitting. The dashed lines in upper diagram indicate broad phase boundaries where the LEED pattern changes continuously.

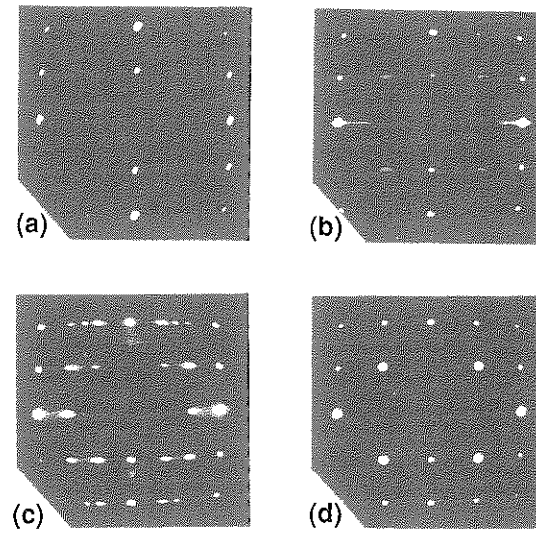

Fig. 2 Typical LEED patterns upon Al deposition onto a single-domain Si(001)2×1 substrate. (a) the clean Si(001)2×1 surface, (b) 0.15 ML at RT, (c) 0.30 ML after annealing of 300°C, (d) 0.50 ML at RT, respectively.

This suggests the formation of 3D islands over an intermediate layer of 1 ML coverage after annealing. The saturation of XPS ratio to the fixed value may be due to the completion of 3D island formation.

Several LEED patterns observed are shown in **Fig. 2**. Figure 2a is a LEED pattern of a clean SD Si(001)2×1 surface. The intensity of a (1, 1/2) spot of the minor-domain is ~1/9 of that of a (1/2, 1) spot of the major-domain. After deposition of 0.1~0.3 ML of Al, long narrow streaks appear along the "×1" direction of the substrate (Fig. 2b). With further deposition, these streaks gradually concentrate around (1/2, 1/2) positions to become sharp (1/2, 1/2) spots of a 2×2 phase at ~0.5 ML (Fig. 2d). This 2×2 pattern persists up to ~2 ML. After post-annealing elongated 2×3 LEED spots appear at 0.1~0.3 ML (Fig. 2c). Around 0.4 ML, two adjacent elongated spots get closer to become "2×5" pattern which is similar to that found for the Ga/Si(001) surface[1, 3, 12]. This "2×5" pattern changes to 2×2 at ~ 0.5 ML, which is almost identical to that of RT. With the increase in Al coverage, however, the 2×2 pattern rapidly weakens and finally becomes 1×1 at ~ 1 ML. The LEED patterns for the 1×1 and 2×2 phases are nearly invariant in the wide ranges of coverage indicated in the upper part of Fig. 1. Upon an increased post-annealing over 350°C, a streaky n×4 phase was found around 0.5 ML instead of 2×2, where "n×" corresponds to the streaky direction and n is around 5. This indicates a very different mode of Al growth at temperatures higher than 350°C in agreement with previous reports[4, 6].

A previous LEED study for a double-domain substrate[4] reported no change in LEED patterns up to ~0.3 ML (below ~0.35 ML at RT), which is different from the present finding of "2×3" and "2×5" phases. The presently found evolution of LEED patterns is almost identical to that of Ga/Si(001)[1, 3, 12]. The evolution of periodicity from 2×3 to 2×5 and to 2×2 for the Ga/Si(001) surface has been generally interpreted[1,3,12] and observed (for 2×3 only) by STM[5, 14] to be as follows. Namely, there are 1D metal-dimer-chains (MDC's) perpendicular to the Si dimer rows. The MDC's can be arranged in the periodicity of 2×3 and 2×5 as coverage of MDC increases, in which the spacing between MDC's is 3a (alternation of 2a and 3a) at ~ 1/3 ML (~ 2/5 ML).

Long streaks along the "×1" direction found at 0.1~0.3 ML at RT (Fig. 2b) can be, thus, interpreted as due to *randomly-spaced* MDC's. As the density of MDC's increases, MDC's are expected to become closer and closer until the whole surface is covered with an ordered arrays of MDC's with 2a spacing at the Al coverage of 0.5 ML. The evolution of LEED

patterns at RT is consistent with this interpretation. This implies that the MDC's are almost immobile at RT until the 2×2 phase is formed. Annealing at 300°C, however, would make the MDC's mobile to rearrange themselves into an ordered 2×3 (or 2×5) array through possible repulsive interaction between them. This can be regarded as an irreversible 1D disorder–order phase transition of the MDC. It is not clear, at this stage, what kind of microscopic motion is involved in the rearrangement of the MDC's.

Very narrow streaks can be seen clearly even at very low coverages of ~0.1 ML indicating that MDC's are very long on the SD substrate. The length (l) of MDC's can be roughly estimated through a relation $\Delta k(\text{Å}^{-1}) \cdot l(\text{Å}) \sim 2\pi$[15] to be longer than 150 Å, where Δk is the width of streaks. This suggest that the mechanism of anisotropic growth, so called 'surface polymerization'[6], is very effective at least for this wide–terrace substrate used. Similar streaks mentioned for In/Si(001) around RT at 0.3 ML[2] can be understood to have the same origin as that of present work. The growth mode up to 2×2 phase for In/Si(001), thus, must be the same as that for Al/Si(001) at RT.

The above results and discussion suggest that there is essentially one mode of growth up to the 2×2 phase of group–III metal on Si(001)2×1. The basic element of the growth mode is the presence of long MDC's formed from very early stage of adsorption. The key factors which affect the mode are (1) the interaction among the MDC's, possibly a short range repulsive interaction, (2) the strength of substrate–adsorbate interaction and (3) the temperature of the system. If the temperature is high enough or if the substrate–adsorbate interaction is weak enough for MDC's to move perpendicularly, the MDC's arrange themselves into the 2×3 or 2×5 structures depending on the density of MDC's. If the condition does not meet, the MDC's would remain randomly spaced to form phases such as 2×1 plus streaks and streaked 2×2 depending on the density of MDC's. The former (the latter) would correspond to the growth of Al at ~300°C and of Ga at RT ~ 500°C (Al at ~RT and In at RT ~ 150°C).

3.2 ARPES results : electronic structure of 232 phase at 0.5 ML

In **Fig. 3** are the ARPES spectra taken along [110] and its symmetrically equivalent line $\bar{\Gamma}_{01}-\bar{J}_{01}-\bar{\Gamma}_{11}$. The measurements along the symmetrically equivalent line including $\bar{\Gamma}_{11}$ instead of the origin of SBZ may be very helpful to determine the dispersions of SS's for two reasons. First, for the Si(001) surface the bulk band gap is much wider around $\bar{\Gamma}_{11}$ than $\bar{\Gamma}_{00}$, thus the SS's can be found much clearly around $\bar{\Gamma}_{11}$. Second, a SS with weak intensity around $\bar{\Gamma}_{00}$ may be found dominantly around $\bar{\Gamma}_{11}$ though the difference in the cross section. In Fig. 3a we can see three SS's denoted as S_1 , S_2 and S_3. S_1 shows

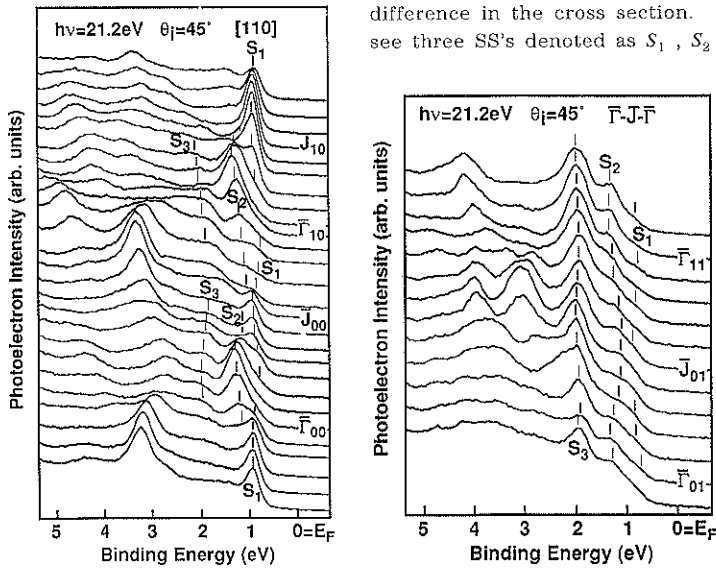

Fig. 3 (a) ARPES spectra taken with synchrotron radiation of $h\nu$ = 21.2 eV along [110]. The incidence angle of photon with respect to surface normal (θ_i) is 45° and the angular step between neighboring spectra is 2°. The corresponding SBZ position is specified by the symmetry symbols (cf. Fig. 4f). The peak positions and assignments of the surface states are marked. (b) Similar to (a), but along the symmetrically equivalent line to [110] axis, i.e., $\bar{\Gamma}_{01}$–$\bar{J}_{01}$–$\bar{\Gamma}_{11}$.

downward dispersion from $\bar{\Gamma}$, where its intensity is very weak. S_2 disperses in an opposite direction from $\bar{\Gamma}$ and gets closer to S_1 near $\bar{J}$. Another SS band S_3, though very weak, can be found at ~2 eV. Along $\bar{\Gamma}_{01}-\bar{J}_{01}-\bar{\Gamma}_{11}$ (Fig. 3b), S_3 is found as a dominant feature showing whole of its dispersion clearly.

In this paper a new method is used for compiling a set of ARPES spectra measured along a axis of SBZ. At first, the raw spectra are normalized by incident photon flux, then the second derivatives with respect to E_B were taken after a smoothing process of spectra. The differentiation is to enhance spectral features. Each of the differentiated spectra is converted to a grey-scale bar, in which intensity is expressed in brightness. The brightness in the bar is, then, roughly proportional to I/W, where I is the intensity of a peak above smooth background and W is the width. The grey-scale bars of a set of ARPES spectra were gathered together into a "grey-scale E_B–$k_{//}$ diagram" where the abscissa is electron wave vector parallel to the surface ($k_{//}$) and the ordinate is E_B[16]. In a grey-scale E_B–$k_{//}$ diagram, one can easily see not only the dispersive behavior of peaks but also their evolution in intensity and width, without any ambiguities of conventional "manual peak-assignment".

In **Figs. 4**a~e, the grey-scale E_B–$k_{//}$ diagrams along five axes of SBZ are shown. The axes are specified by the symbols of SBZ in Fig. 4f. White broken lines are the edges of bulk valence bands projected onto the 1×1 SBZ. The SS-dispersions assigned by comparative inspection of the grey-scale diagrams and raw spectra are drawn with black broken lines.

The diagrams in Figs. 4a~b are for the raw spectra shown in Fig. 3. In these two diagrams we can see three SS's assigned as S_1, S_2 and S_3 in Fig. 3. S_1, S_2 are located inside the bulk band gap around $\bar{\Gamma}_{10}$.

In Figs. 4c~d are the diagrams for the scan along symmetrically equivalent directions of $\bar{\Gamma}-\bar{J}'-\bar{\Gamma}$. We can find S_1 and S_2 with very similar dispersions as along $\bar{\Gamma}-\bar{J}-\bar{\Gamma}$ direction (Figs. 4a~b). The dispersion of S_2, however, shows two branches denoted as S_2 and S'_2. The upper branch S_2 shows an upward-dispersion from $\bar{\Gamma}_{10}$ to $\bar{J}'_{10}$ and becomes very weak over $\bar{J}'_{10}$. The lower part S'_2 splits from S_2 near $\bar{\Gamma}$ and disperses downward and then, "degenerates" (within the experimental resolution of ~150 meV) again at $\bar{J}'$. S_3 band shows a large upward dispersion from $\bar{\Gamma}$ to $\bar{J}'$ in Fig. 4c but a split band, S'_3 can be found in Fig. 4d. S'_3 seems to disperse in downward direction from $\bar{\Gamma}_{11}$ to $\bar{J}'_{10}$. S_3 and S'_3 have a splitting of ~ 0.5 eV at $\bar{J}'$. Because the bulk band gap extends to much larger E_B's than 2 eV around $\bar{\Gamma}_{11}$ (cf. Fig. 4e), S_3 (S'_3) also has some part

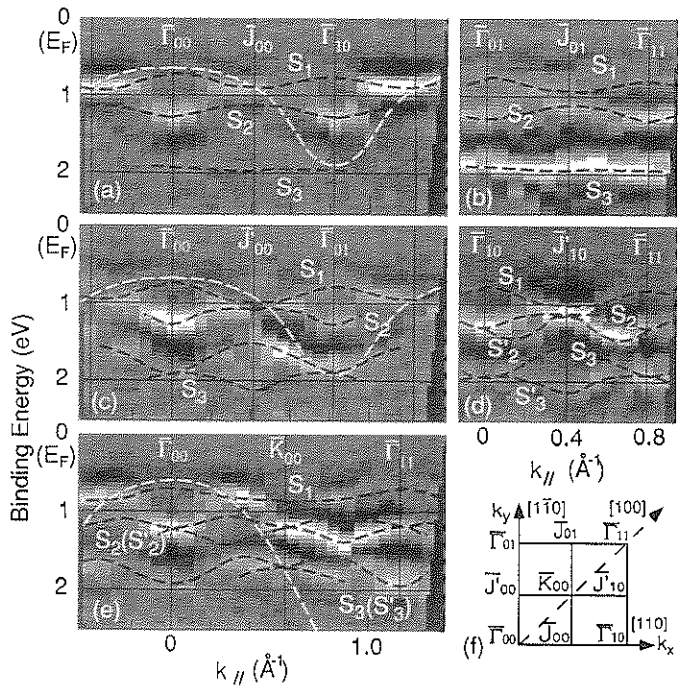

Fig. 4 (a)~(e) Grey-scale E_B–$k_{//}$ diagrams for the Si(001)2×2-Al surface along the marked symmetric axes of the 2×2 surface Brillouin zone (SBZ). (f) SBZ of Si(001)2×2-Al surface with symbols of relevant symmetric points. The "2×" direction of the substrate 2×1 is along [110] (k_x) and $\bar{\Gamma}_{01}$ corresponds to $\bar{J}'$ of the 2×1 SBZ. Diagrams (a) and (b) ((c) and (d)) are for the symmetry-identical direction of $\bar{\Gamma}$–$\bar{J}$ ($\bar{\Gamma}$–$\bar{J}'$). Brief explanation of grey-scale E_B–$k_{//}$ diagram is in the text.

of their band inside the bulk band gap. This fact supports that all the five bands, S_1, S_2, S'_2, S_3 and S'_3, are SS's. This was further confirmed from the invariance of their E_B to photon energy[17].

In the grey-scale diagram along [100] axis in Fig. 4e, we can also find five SS's. S_1 is found to have a similar dispersion following the 2×2 periodicity as along the other two directions. Since we know already that S_2 band is composed of two states with proper symmetry of 2×2 SBZ, the dispersion of S_2 should be the one shown in Fig. 4e according to the symmetry of SBZ. Likewise, a similar two-branch structure can be deduced for S_3 as in Fig. 4e, although the dispersion of the lower branch around $\bar{\Gamma}$ is unclear.

The dispersions of SS's along the two edges of SBZ, $\bar{J}'_{00}-\bar{K}_{00}-\bar{J}'_{10}$ and $\bar{J}_{00}-\bar{K}_{00}-\bar{J}_{01}$ were also determined through similar procedure. Along $\bar{J}'_{00}-\bar{K}_{00}-\bar{J}'_{10}$, S_3 and S'_3, which have large splitting at $\bar{J}'$, get closer toward $\bar{K}$ and finally degenerate at $\bar{K}$ in consistent with the result of Fig. 4e. No evidence for splitting of both S_2 and S_3 along $\bar{J}_{00}-\bar{K}_{00}-\bar{J}_{01}$ direction is found[17].

Figure 5a summarizes the dispersions of five SS's. The unclear parts of dispersions are drawn tentatively with broken lines. The squares and circles (open and closed) are the previous reports for the dispersions of SS's of a single-domain Si(001)2×2-Ga[12] and a double-domain Si(001)2×2-In [7] surfaces, respectively, which will be discussed later. The five SS's run nearly parallel to each other all over the SBZ. The dispersion of S_1 is quite isotropic around $\bar{\Gamma}$, while those of S_2 (S'_2) and S_3 (S'_3) are anisotropic around $\bar{\Gamma}$. S_2 and S'_2 degenerate along $\bar{\Gamma}-\bar{J}-\bar{K}-\bar{J}'$ and S_3 and S'_3 degenerate along $\bar{\Gamma}-\bar{J}-\bar{K}$. S_3 (S'_3) shows a largest amount of dispersion, 0.4 eV, from $\bar{K}$ to $\bar{J}'$.

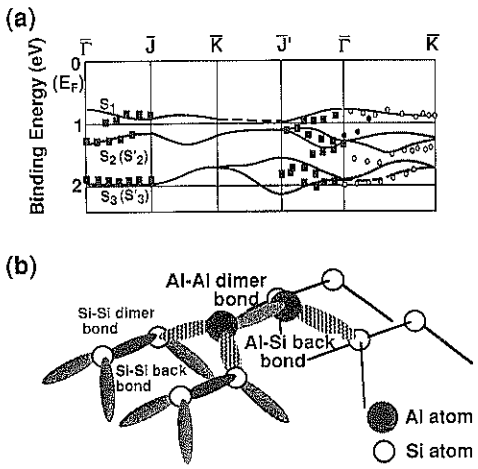

Fig. 5(a) Summary of the dispersions of five surface states assigned for the Si(001)2×2-Al surface. Parts of dispersions drawn with broken lines are tentative. The dispersions of SS's for the Si(001)2×2-In[7] and -Ga[12] are given for comparison with circles (open and closed) and squares, respectively. The open (closed) circles are taken from the scan between $\bar{\Gamma}_{11}$ and $\bar{K}_{00}$ (around $\bar{\Gamma}_{00}$) of ref. 8. (b) Schematic illustration of atoms and bonds in the 2×2 unit cell for the parallel dimer model[5,7].

In the structural models for 2×2 phase of Al, Ga and In considered so far, there are two Si-dimers and one metal-dimer bonded to the Si-dimers in each 2×2 unit cel[5,7]. These models have 10 electrons in each surface unit cell, 6 from two metal atoms (s^2p) and 4 from the otherwise dangling bonds of Si-dimers. These electrons form four back-bonds between four Si-dimers and an adsorbate dimer and one adsorbate dimer-bond within the metal dimer (see Fig. 5b), which result in five fully-occupied SS's. The SS due to adsorbate dimer-bond is expected to have less E_B than back-bonds, because an metal dimer bonding is weaker than an metal-Si covalent bonding due to the electronegativity difference of metal and Si. The SS's from the back-bonds may degenerate into one or two states due to the identical configuration of the four back-bonds. This expectation agrees very well with five SS's found in the present work and the fact that four of them with higher E_B degenerate into two states at some parts of SBZ. Thus it may be plausible to assign the band S_1 as the state due to a dimer-bond and S_2 (S'_2) and S_3 (S'_3) as due to the back-bonds. Less-dispersive nature of S_1 also agrees with the notion that a dimer-bond orbitals are isolated. The anisotropic dispersion of S_2 (S'_2) and S_3 (S'_3), then, may reflect the difference in the amount of coupling of wave functions along [110] and [1$\bar{1}$0] directions in terms of tight binding idea (Fig. 5b).

The surface electronic structure of a single-domain Si(001)2×2-Ga surface was studied by Enta et al.[12] with ARPES using a rare-gas resonant lamp along [110] and [1$\bar{1}$0] directions (see the squares of Fig. 5a). Along [110], three SS's were found whose dispersions are almost the same as those of S_1, S_2 and S_3 of the present work. Along [1$\bar{1}$0], three SS's were also found[12] but the expected 2×2 periodicity for the state corresponding to S_2 was not found. This discrepancy can be solved by the existence of two split states for S_2 with proper 2×2 periodicity in the present work. The dispersion of third state was almost the same as that of S_3, though its splitting was not noticed before[12].

Another ARPES study was done on a double-domain Si(001)2×2-In surface along the common axis <100> of the two domain[7]. The authors found three SS's, denoted as S_1, S_2 and S_3 between $\bar{K}_{00}$ and $\bar{\Gamma}_{11}$ and compared the dispersions with their theoretical calculation based on a parallel dimer model. The

dispersions of these states are quite similar to those of S_1, S_2 and S_3 in our work, except for the absence of the upper branches of S_2 and S_3 (cf. Fig. 5a). The uncertainty of S_1 band near $\overline{\Gamma}_{00}$ mentioned in ref. 7 can be resolved if the lower part of peaks near $\overline{\Gamma}$ (closed circles in Fig. 5a) corresponds to S_2 band in the present work. Though it was argued that the results of calculation agree well with the experiments[7], it is questionable from our finding of two additional SS's for the 2×2–Al surface. We think that it is desirable to calculate the SS dispersions in detail for both the parallel and perpendicular dimer models in order for better comparison to our new result.

4. Summary

LEED and XPS were applied to the adsorption of Al on a wide–terrace single–domain Si(001)2×1 surface. Modes of Al growth were tested for two temperature conditions of the substrate, one around RT and the other at 300°C. A rich sequence of LEED patterns as summarized in Fig. 1 is observed. It was determined that the 2×2 phase completes at 0.5 ML. Long and narrow streaks pointing toward "×1" direction were found for the first time at RT in coverages 0.1~0.45 ML. This indicates that metal–dimer chains are randomly arranged at RT for Al coverages 0.1~0.45 ML. The presence of "2×3" and "2×5" phases found after annealing indicates that the MDC's are almost regularly arranged through disorder–order transition of 1D MDC's due to increased mobility of MDC's at 300°C and possible repulsive interaction among MDC's. The mode of formation for the 2×2 at 300°C is essentially identical to that of Ga/Si(001) at RT~500°C. The mode of formation at RT is similar to that of In/Si(001) at RT~150°C. Thus, the growth modes of Al, Ga and In on Si(001) up to the 2×2 phase are consistently understood in terms of the disorder–order transition of 1D MDC's.

ARPES study using synchrotron radiation has been performed on a single–domain Si(001)2×2–Al surface in order to elucidate the surface electronic structure. Through detailed ARPES measurements for various lines of SBZ, we have identified the presence and dispersions of five SS's, one (S_1) just less than 1 eV and the others (S_2, S'_2, S_3 and S'_3) between 1 eV and ~ 2 eV in E_B. The latter four states appeared to degenerate into two states in some parts of SBZ. From the characteristics of their dispersions, it is tentatively inferred that S_1 is due to the Al–Al dimer bond and S_2 (S'_2) and S_3 (S'_3) to the Al–Si back–bonds of the Al–dimer models. However, the exact assignment of the origins of these SS's remains to be confirmed by an ab–initio calculation of surface electronic structures.

Acknowledgements

The authors are grateful to Drs. K. Sakamoto and T. Sakamoto of Electrotechnical Laboratory for providing us with a well–oriented Si wafer. Parts of this work was performed under the Photon Factory proposal number of 94–G189.

References

1) T. Sakamoto and H. Kawanami : Surf. Sci. **111**, 177 (1981).
2) J. Knall, J. –E. Sundgren, G. V. Hansson and J. E. Greene : Surf. Sci. **166**, 512 (1986).
3) B. Bourguignon, K. L. Carleton and S. R. Leone : Surf. Sci. **204**, 455 (1988).
4) T. Ide, T. Nishimori and T. Ichinokawa : Surf. Sci. **209**, 335 (1989).
5) J. Nogami, A. A. Baski and C. F. Quate : Phys. Rev. **B 44**, 295 (1991) and references therein.
6) G. Brocks, P. J. Kelly and R. Car : Phys. Rev. Lett. **70**, 2786 (1993).
7) J. E. Northrup, M. C. Schabel, C. J. Karlsson and R. I. G. Uhrberg : Phys. Rev. **B 44**, 13799 (1991).
8) H. Sakama, K. Murakami, K. Nishikata and A. Kawazu : Phys. Rev. **B 48**, 5278 (1993) ; Phys. Rev. **B 50**, 14977 (1994).
9) B. E. Steele, L. Li, J. L. Stevens and I. S. T. Tsong : Phys. Rev. **B 47**, 9925 (1993).
10) H. Itoh, J. Itoh, A. Schimid and T. Ichinokawa : Phys. Rev. **B 48**, 14663 (1993) ; Surf. Sci. **302**, 295 (1994).
11) Y. Qian, M. J. Bedzyk, S. Tang, A. J. Freeman and G. E. Franklin : Phys. Rev. Lett. **73**, 1521 (1994).
12) Y. Enta, S. Suzuki and S. Kono : Surf. Sci. **242**, 277 (1991) ; Y. Enta : Ph. D. Thesis, Tohoku University, Japan (1990).
13) T. Abukawa, T. Kashiwakura, T. Okane, Y. Sasaki, H. Takahashi, Y. Enta, S. Suzuki, S. Kono, S. Sato, T. Kinoshita, A. Kakizaki, T. Ishii, C. Y. Park, S. W. Yu, K. Sakamoto and T. Sakamoto : Surf. Sci. **261**, 217 (1992).
14) A. A. Baski, J. Nogami and C. F. Quate : J. Vac. Sci. Technol. **A8**, 245 (1990).
15) M. Henzler : Surf. Sci. **152/153**, 963 (1985).
16) T. Abukawa, M. Sasaki, F. Hisamatsu, T. Goto, T. Kinoshita, A. Kakizaki and S. Kono : Surf. Sci. **325**, 33 (1995)
17) H. W. Yeom, T. Abukawa, Y. Takakuwa, M. Nakamura, M. Kimura, A. Kakizaki and S. Kono : Surf. Sci. **321**, L177 (1994).